# Modeling of Capillary Sealing Fractures during CO2 Injection by Non-Matching Multi-block Grids

Mohammed Adil Sbai

XVIII International Conference on Water Resources
CMWR 2010
J. Carrera (Ed)


# MODELING OF CAPILLARY SEALING FRACTURES DURING $CO_2$ INJECTION BY NON-MATCHING MULTI-BLOCK GRIDS

**Adil M. Sbai***

*BRGM, Water Division
3, Avenue Claude Guillemin, BP 36009, 45060 Orléans CEDEX 2, France.
e-mail: a.sbai-AT-brgm.fr, web page: http://www.brgm.fr/

**Key words:** $CO_2$ injection, Local grid refinement, Fractured media, Two-phase flow

**Summary.** Among open scientific challenges facing large scale implementation of $CO_2$ sequestration, are geological structures at different scales not properly dealt with at the injection scale. Faults and fractures, in particular, could have large impacts on the flow dynamics and $CO_2$ leakage to the atmosphere. In order to give a full 3D representation to these sensitive zones we present an approach for simulating multiphase fluid flow on non-overlapping, non-matching, multi-block grids. Capillary pressure and relative permeability properties of fault zones are explicitly taken into account in this approach. The underlying technique was implemented in the framework of a domain decomposition leading to development of a multilevel multigrid iterative scheme. Different interpolation methods between the coarse and fine grids in the fault zones have been tested leading to an improved implicitness, and thus allowing larger time step sizes to be taken. Results of numerical experiments for a simplified, but computationally demanding reservoir models are presented.

## 1 INTRODUCTION

While the number of field tests of $CO_2$ storage in deep saline aquifers and depleted hydrocarbon reservoirs is growing considerably during the last years, its appraisal at large scale in sedimentary basins rises fundamental scientific concerns [6]. Among these, questions like "What would be the mass fraction of gaseous or supercritical $CO_2$ at the exit of a fault zone after many years of injection?" or "How uncertainties in intrinsic properties of these faults do impact capacity and storage effectiveness, or leakage flux to overlying freshwater aquifers, if any?" have not been discussed on a wide breadth. Some of reported numerical modeling studies have tackled the problem from a codes benchmarks perspective to establish confidence in available simulation techniques [3]. Other approaches fairly simplify the domain geometry, by considering explicitly the fault as a single domain, favoring a study of advanced non-isothermal multiphase leakage processes [9]. Recently,

detailed geometrical features of the aquifer have been considered in geological modeling of the Johansen formation by [4] but they do rely on the common-place transmissibility multipliers approach to assign fault properties. The later approach is usually effective for single-phase flow to approximate rock and fluid properties across low-dimensional fault surfaces from neighboring cells. In [7] two phase flow transmissibility multipliers are derived. As a general rule, $CO_2$ multiphase flow processes require fine scale permeability, relative permeabilities, and capillary pressure properties to be assigned to fault zones explicitly.

The main goal of this paper is to investigate this explicit modeling approach around a single three-dimensional fault zone. We focus, in this work, on a local grid refinement technique (LGR) leading to an overall reduction of the unknowns resulting from fine discretisation in these zones. A detailed study of the underlying physics when taking this approach into account will not be considered herein. The later requirements related to quantitative modeling will be investigated thoroughly in future research studies. Thus, we aim to include the detailed geometry and material properties of the fault, while its immediate surroundings is best represented as an equivalent porous medium whose properties might be deduced through upscaling of fractured networks. To allow for such complex modeling we avoid discretization on conforming meshes directly.

In this presentation reduction of the computational burden is achieved through a domain decomposition. The latter splits the governing equations among smaller sub-domains to be solved independently. Mass conservation along non matching interfaces of different subdomains is iteratively found with a two-level Multigrid like solver. The numerical scheme ensures convergence of the usual Newton-Raphson iteration and the composite grid iteration simultaneously.

The following section briefly introduces the governing equations used by our numerical model. Next, the main steps taken in the implementation of the LGR technique and the two-level solver are presented. The fourth section demonstrates the application of the developed procedure to a hypothetical heterogeneous and anisotropic saline aquifer involving both layered and structural heterogeneities. Then we end up with conclusions, possible extensions of this modeling approach, and its application to different areas in $CO_2$ sequestration science.

## 2 MATHEMATICAL MODEL

When carbon dioxide remains as a supercritical phase, it can be considered as a slightly compressible fluid. Under these assumptions, the governing two-phase fluid flow motion equations are expressed using a coupled system of global pressure and phase saturation equations given by [2, 5]

$$\phi c_t \frac{\partial p}{\partial t} = \nabla . \left[ \mathbf{k} \lambda_t \left( \nabla p - \left( f_w \rho_w + f_c \rho_c \right) g \nabla z \right) \right] + \frac{q_w}{\rho_w} + \frac{q_c}{\rho_c} \tag{1}$$

$$\frac{\partial\left(\phi S_c\right)}{\partial t} = -\nabla.\left[\mathbf{k} f_c \lambda_w \left(\frac{dp_c}{dS_c}\nabla S_c - \Delta\rho g \nabla z\right) + f_c \mathbf{u}\right] + \frac{q_c}{\rho_c} \tag{2}$$

Where $c_t$ is the total compressibility of the fluid and rock system, $\phi$ is the rock porosity, $p$ is the fluid pressure, $\lambda_t = \lambda_w + \lambda_c$ is the total mobility, $\lambda_l = \frac{k_{rl}}{\mu_l}$ is the relative permeability, $k_{rl}$, of phase l=(w:water, c:$CO_2$) to its viscosity, $\mu_l$, ratio; $\mathbf{k}$ is the principal intrinsic permeability tensor of the porous medium, $S_c$ is the saturation of $CO_2$ fluid phase, $f_l = \frac{\lambda_l}{\lambda_t}$ is the fractional flow function of phase l, $\mathbf{u} = \mathbf{u}_w + \mathbf{u}_c$ is the total fluid flow velocity, $p_c$ is the capillary pressure, $\rho_l$ is the density of fluid phase $l$, $\Delta\rho = \rho_w - \rho_c$ is the difference between densities of $CO_2$ and aqueous phases respectively, $q_l$ is the time-dependent total injection/withdrawal term of phase $l$, $\nabla = \left(\frac{\partial}{\partial x}, \frac{\partial}{\partial y}, \frac{\partial}{\partial z}\right)$ is the partial differential operator, $t$ is time, $g$ is the z-axis component of the gravity vector $\mathbf{g} = (0, 0, -g)^T$ directed downward. The transport equation for dissolved non-reactive $CO_2$ species in the aqueous phase, including fluid advection and macro-dispersion effects [1], is

$$\phi\frac{\partial\left(1 - S_c\right)C}{\partial t} = -\nabla.\left(C\mathbf{u}_w\right) + \nabla.\left(\phi\mathbf{D}\nabla C\right) + \rho_c T_d \tag{3}$$

Where C is the concentration of $CO_2$ in the aqueous phase, $\mathbf{D}$ is the dispersion tensor, and $T_d$ is the mass transfer by the dissolution mechanism which could be reasonably approximated for a range of subsurface temperature and pressure conditions by a lumped thermodynamic model. Equations 1, 2 and 3 are supplemented by closure relationships for rock and fluid equation of state properties [2], such as saturation dependent relative permeabilities, $k_{rl}(S_w)$, and capillary pressure, $p_c(S_w)$, curves.

## 3 MODELING CONCEPTS AND NUMERICAL IMPLEMENTATION

It is well known that the discretization of equations 1, 2 and 3 as a coupled set leads to a non-linear set of equations, regardless of the numerical method used [2]. These equations are solved directly with a Newton-Raphson iteration or through Newton-like linearization methods. One class of the latter methods involves decoupling the equations by dropping all cross-derivative terms in the Jacobian matrix leading to a sequential iteration scheme. The solver presented in this work is independent on the coupling scheme, it involves only access to the system Jacobian as discussed further in the text.

### 3.1 Local grid refinement

Our choice of LGR technique for simulation of $CO_2$ storage applications stands on previous experiences associated with difficulties to optimize the mesh size for three-dimensional problems [3]. Refinement is generally required in the vicinity of injection wells, very permeable structures, or highly heterogeneous zones. Implementation of the technique enable us first to reduce the problem size to a bear minimum. Second, coarse cells decomposition allow for independent numerical solutions in refined subdomains which enhances accuracy and reduces memory usage. Notice also that a parallel implementation based

on this approach is quite straightforward.
We start by defining a coarse and possibly irregular grid, $\Omega_c$, which is matching at all interfaces. Then any coarse cell in this grid might be irregularly decomposed in 3-D space, if needed, to build a fine subdomain $\Omega_i$. To allow for greater flexibility, each of these subdomains have its own level of refinement independently on the others. Therefore we end up with a composite grid, $\Omega = \Omega_c + \cup_{i=1}^{N_i} \Omega_i$ consisting of some coarse cells and all refined subdomains. This composite grid is non-matching at some interfaces and non-regular, this is known as multi-block data structure.

### 3.2 Numerical scheme

We apply the fast composite adaptive method introduced by [8, 10] for local refinement to the following nonlinear system of equations in the composite grid $\Omega$

$$J^n \Delta X^{n+1} = b^n \tag{4}$$

Where $J^n$ is the system Jacobian at time level $n$. In this numerical scheme the composite solution is sought by a two-level iteration between fine and coarse partitions. It can be envisioned as a Multigrid scheme which, in its principles, uses the error approximation in the coarse grid to iteratively update the composite solution.
We consider the restriction and prolongation operators $R$ and $R^T$ to map solution vectors between the composite grid and the coarse grid, respectively. The Later is nothing else than an interpolation from the coarse to the composite grid. Another restriction operator, $S_i$, maps the solutions from the composite grid to fine subdomain $\Omega_i$, such that $X_{\Omega_i} = S_i X$. Notice that combination of operators $S_i$ and $R^T$ leads to definition of another mapping operator, $R_i^T = S_i R^T$ from the coarse grid to the fine subdomain $\Omega_i$.
Denoting the Newton iterate in equation 4 by $X^{n,m}$ and the solution increment as

$$\Delta X^{n,m} = X^{n,m} - X^n \tag{5}$$

the composite problem, at Newton iteration step m, turns out to be

$$J^n \Delta X^{n,m} = b^n \tag{6}$$

An intermediate iterate $X^{n,m+1/2}$ is defined as the sum of the previous solution to the linear system of equations 6 and an interpolation of a coarse grid correction calculated at iterate m, $C^m$, onto the composite grid. That is

$$X^{n,m+1/2} = X^{n,m} + R^T C^m \tag{7}$$

Substitution of equation 7 into equation 6 and application of the restriction operator to the coarse grid yields the equation

$$R J^n R^T C^m = R(b^n - J^n \Delta X^{n,m}) \tag{8}$$

The right hand side in the coarse equations is nothing else than the restriction of the composite grid residual to the coarse grid $\Omega_c$. The later remark simplifies also implementation in computer programming.
Once the coarse scale equations 8 are solved, coarse solution vector, $X_{\Omega_c}^{n,m+1}$, at iterate $m+1$ is updated according to the following equation

$$X_{\Omega_c}^{n,m+1} = X_{\Omega_c}^{n,m+1/2} = X_{\Omega_c}^{n,m} + R_c^T C^m \tag{9}$$

On the other hand, fine subdomain solution vectors, $X_{\Omega_i}^{n,m+1/2}$, are updated at intermediate iteration level $m+1/2$

$$X_{\Omega_i}^{n,m+1/2} = X_{\Omega_i}^{n,m} + R_i^T C^m \quad i = 1, ..., N_p \tag{10}$$

The latter solution is taken as new boundary conditions in all fine subdomains. We next update Newton increments, at the fine scales, by solving in all subdomains

$$J_{ii} \Delta X_{\Omega_i}^{n,m+1} = b_{\Omega_i}^n - \sum_{j \neq i} J_{ij}^n \Delta X_{\Omega_j}^{n,m+1/2} \quad i = 1, ..., N_p \tag{11}$$

where $J_{ij}^n$ is the contribution from the neighbor subdomain j to i$^t h$ non-matching boundary ensuring flux continuity requirement. This two-level iteration proceeds until a given stopping criteria norm is satisfied for the composite solution vector. This is taken herein as the relative error norm

$$\frac{||X^{n,m+1} - X^{n,m}||}{||X^{n,m}||} < \epsilon \tag{12}$$

where $\epsilon$ is a predefined tolerance usually in the range between $10^{-5}$ and $10^{-9}$.
The numerical scheme presented in this paragraph has been implemented as an independent object oriented mathematical toolbox in MATLAB software to promote reuse for other applications. Next to this first proof-of-concept stage we plan a port to a high level computer language, such as C++, for much greater efficiency and portability to other computer platforms.

## 4 NUMERICAL RESULTS

The LGR technique and two-level solver presented previously have been applied to simple theoretical one- and two-dimensional problems. These results are not reported here for compactness, but will be given in upcoming publications. The numerical model is shown to be applied directly to a full three-dimensional test case according to our initial objectives.

We consider a global simulation domain of 1000x200x150 m$^3$ size. Two fault zones, parallel to x-axis, with a lateral extension of 20 meters each, separate three stratigraphic heterogeneous and anisotropic layers of 30 meters depth. Fault mid-planes are located at

400 and 500 meters from the downstream left boundary and have vertical drops of 20.2 and 95.5 meters, respectively (Fig. 1). The top surface of the deeper stratigraphic layer is 2000 meters deep. The three permeable layers are sandwiched between clayey zones which are coarsened 10 times in all directions. The final composite grid have only 23280 cells among which 23200 are in the fine zones. A uniform cell size of 10x10x3 $m^3$ in the five zones of interest is selected to allow for a geostatistical description of the layered and structural heterogeneities.

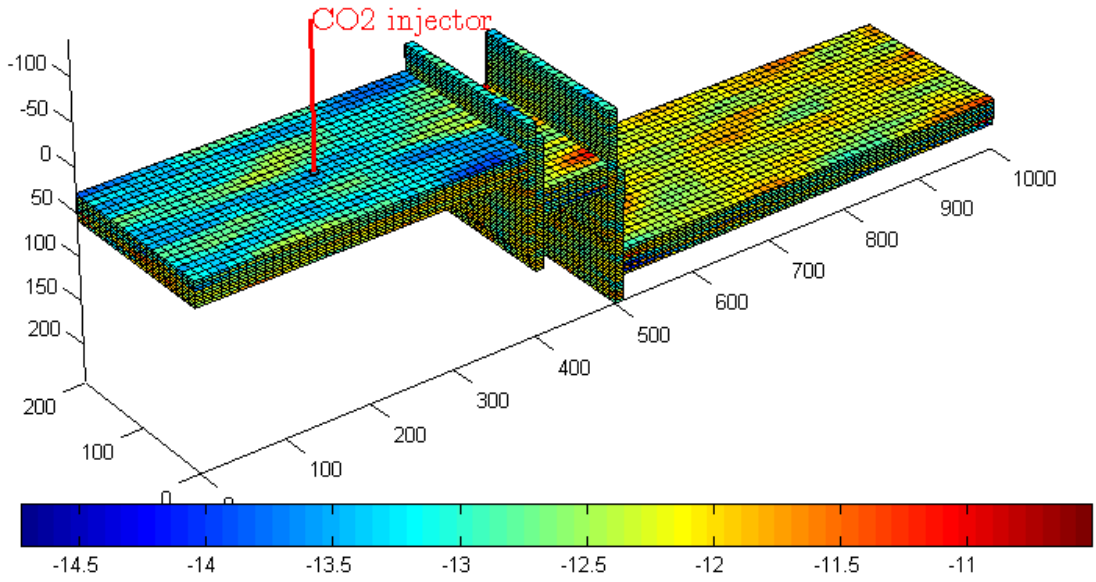


Figure 1: Permeability distributions in the three faulted blocks and the two fault zones of the problem test case (plotted values are in Log-scale).

The permeability distribution shown in figure 1 is assumed to follow a simple log-normal distribution in each layer of the three stratigraphic units and fault zones. Fluids densities and viscosities are hold constants during the simulation and simple quadratic power law relative permeability laws are selected. A constant pressure boundary condition equal to 200 bars is attributed to the downstream surface, parallel to x-axis, in the third faulted block, while all other boundaries are closed. $CO_2$ is injected at a constant rate of 70 t/day during all 3000 days of the simulation period.
Figure 2 shows distribution of $CO_2$ saturations during later times (2500 and 3000 days) for two cases. The only difference between the two simulations is the capillary function attributed to the fracture zones. In the first case, $CO_2$ leakage at the top boundaries of the fracture cells is quite apparent, hindering storage effectiveness. In the second case, capillary pressure forces in fractures exceed buoyant gravity forces, such that $CO_2$ flows underneath and continue its migration in other stratigraphic blocks. We notice also a

longer extension of the plume in the second case demonstrating a much higher storage efficiency. Hence, our simulations highlight sensitivity of faults two-phase flow properties with regards to sequestration capacity and security simultaneously. Our future simulation efforts will focus on model applications to more realistic scenarios inspired from natural analogues of oil and gas reservoirs showing accumulations near faulted zones.

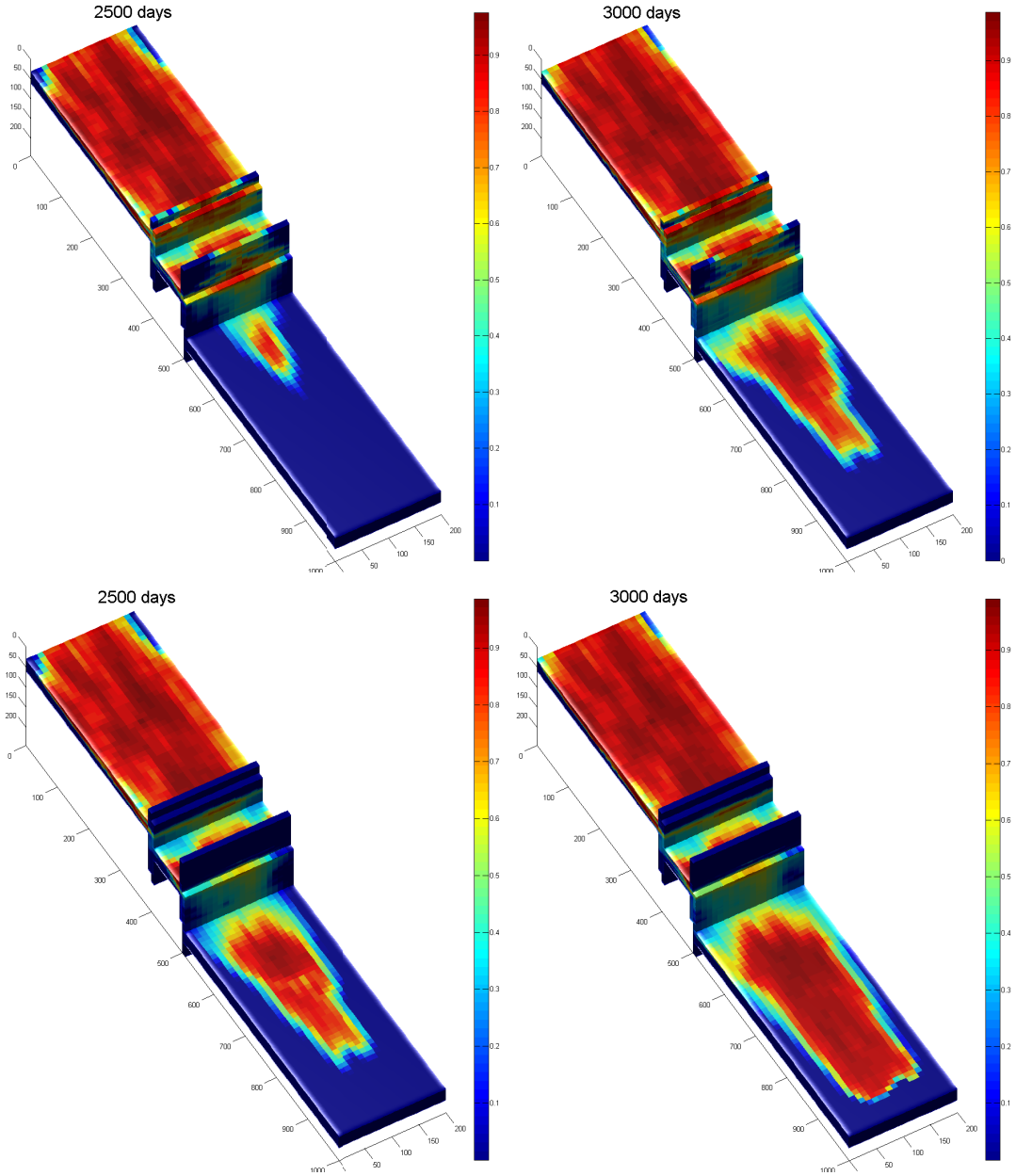


Figure 2: $CO_2$ saturation maps after 2500 and 3000 days of injection for case 1 (top) and case 2 (bottom).

## 5 CONCLUDING REMARKS

This work had presented an approach for numerical modeling of two-phase flow problems in faulted reservoirs. Structural and layered heterogeneities may be combined explicitly and thus allowing to undertake much comprehensive simulations on full-scale realistic geological models. A local grid refinement technique leading to a two-level multigrid solver substantially reduce the computational requirements and shows to be effective for $CO_2$ storage simulations. Our future research work involves applications to natural analogues and refinement of multiphase processes taken into account by the numerical simulator.

**Acknowledgments** This research work is supported by the French Research Council (ANR), under contract number ANR-06-CO2-006-01 in the framework of HETEROGENEITES-$CO_2$ project initiative.

## REFERENCES

[1] J. Bear and Y. Bachmat. *Introduction to modeling of transport phenomena in porous media*, Kluwer Academic Publishers, (1990).

[2] Z. Chen, G. Huan, and Y. Ma. *Computational methods for multiphase flows in porous media*, SIAM, (2006).

[3] H. Class, et al. A benchmark study on problems related to $CO_2$ storage in geologic formations. *Comput. Geosc.*, **13**(4), 409-434, (2009).

[4] G.T. Eigestad, H. K. Dahle, B. Hellevang, F. Riis, W.T. Johansen, and E. ian. Geological modeling and simulation of $CO_2$ injection in the Johansen formation. *Comput. Geosc.*, **13**(4), 435-450, (2009).

[5] R. Helmig. *Multiphase flow and transport processes in the subsurface*, Springer, (1997).

[6] IPCC. *Carbon Dioxide Capture and Storage*. Bert Metz, Ogunlade Davidson, Heleen de Coninck, Manuela Loos and Leo Meyer (Eds.) Cambridge University Press, UK. pp 431, (2005).

[7] T. Manzocchi, A. E. Heath, J. J. Walsh and C. Childs. The representation of two phase fault -rock properties in flow simulation models. Petroleum Geosc., **8**, 199-132, (2002).

[8] S. McCormick and J. Thomas. The fast adaptive grid composite method for elliptic boundary value problems. *Mathematics and Computing*, **46**, 438–456, (1986).

[9] K. Pruess. Thermal effects during $CO_2$ leakage from a geologic storage reservoir. Lawrence Berkeley National Laboratory, Report LBNL-55913, (2004).

[10] R. Teigland. On some variational acceleration techniques and related methods for local refinement. *Int. J. Num. Meth. Fluids*, **28**, 945–960, (1998).